



Published in final edited form as:

Regen Med. 2014 January ; 9(1): 41–51. doi:10.2217/rme.13.76.

## Injectable gel graft for bone defect repair

Josephine Fang<sup>1</sup>, Zhi Yang<sup>1</sup>, ShihJye Tan<sup>2</sup>, Charisse Tayag<sup>1</sup>, Marcel E Nimni<sup>1</sup>, Mark Urata<sup>1</sup>, Bo Han<sup>\*,1,2</sup>

<sup>1</sup>Division of Plastic & Reconstructive Surgery, Department of Surgery, Keck Medical School, University of Southern California, 1333 San Pablo St, BMT 302A, Los Angeles, CA 90089-9112, USA

<sup>2</sup>Department of Biomedical Engineering, Viterbi School of Engineering, University of Southern California, Los Angeles, CA, USA

### Abstract

**Aim:** To examine the performance of an injectable gel graft made of transglutaminase (Tg)-crosslinked gelatin gel with BMP-2 (BMP-2–Tg–Gel) for bone defect repair in animal models.

**Materials & methods:** BMP-2 mixed with gelatin gel was crosslinked using Tg. The release of tethered BMP-2 through autocrine and paracrine pathways was demonstrated by using C2C12 and NIH 3T3 cells, respectively. BMP-2–Tg–Gel was injected into the induced cranial defect site. After 14 days, the sample was removed for x-ray imaging and histological evaluation.

**Results:** Our *in vivo* results demonstrated that the injectable Tg–Gel with its osteoconductivity and controllable BMP-2 activity induced bone formation in our rat models when tethered with BMP-2.

**Conclusion:** Tg–Gel as an injectable functional bone graft may enable the use of minimally invasive surgical procedures to treat irregular-shaped bone defects. Furthermore, this novel approach is capable of incorporating and controlling the release of therapeutic agents that may advance the science of tissue regeneration.

### Keywords

BMP-2 delivery; bone defect repair; gelatin gel; injectable; osteoconductive; osteogenic; transglutaminase

---

Although bone autograft implantation is routinely used to heal critical bone defects due to its osteoconductive and osteogenic properties, healing bone defects caused by trauma, tumors, or developmental and congenital causes still remains a major concern in

---

For reprint orders, please contact: reprints@futuremedicine.com

\*Author for correspondence: Tel.: +1 323 442 2242, Fax: +1 323 442 5956, bohan@usc.edu.

**Publisher's Disclaimer:** Disclaimer

The contents are solely the responsibility of the authors and do not necessarily represent the official view of the NIH.

Ethical conduct of research

The authors state that they have obtained appropriate institutional review board approval or have followed the principles outlined in the Declaration of Helsinki for all human or animal experimental investigations. In addition, for investigations involving human subjects, informed consent has been obtained from the participants involved.

reconstructive surgery. Long-term outcome in craniofacial reconstruction using autologous bone grafts is unreliable because of bone resorption. In addition, decreased spontaneous bone healing capacity of children aged 2–10 years poses significant difficulties due to lack of enough autologous bone volume [1,2]. Limited graft quantity and donor site morbidity have intensified and instigated the development of improved methods for bone regeneration. Therefore, the use of scaffolds for cells and growth factor delivery has drawn a considerable amount of interest in bone restoration. There are various materials such as cement pastes, osteoconductive and osteoinductive biomaterials, and prefabricated polymers that have been investigated for craniofacial reconstruction and augmentation. Ideally, the scaffold for bone regeneration should be biocompatible, osteoconductive and osteoinductive, nonimmunogenic, and mechanically strong while maintaining its elasticity [3].

Calcium phosphate cements offer several advantages such as ease of placement using injections, ability to withstand compression and formation of chemical bonds with bone [4–6]. However, previous studies have shown that cell migration and remodeling of this scaffold after long periods is minimal, resulting in poor assimilation into bone. Other complications include disintegration of material due to meningeal pulsatile forces, suggesting its inability to withstand dynamic shear force. Demineralized bone matrix allografts implanted using various carriers such as glycerol (Grafton; Osteotech, CA, USA) have been studied and have shown evidence of healing of critical size defects in as little as 12 weeks [7]. Similarly, InterGro (Biomet, IN, USA), a demineralized bone matrix/lecithin composite has been discovered to possess optimized osteoinductive properties in a previous study [8]. Nonetheless, these materials are non-settable and display weak mechanical properties. Hence, they do not provide any immediate protection to the brain [7].

A promising alternative to autografting is BMP-2, which induces osteogenesis to repair bone defects and serves as the basis for tissue engineering. Absorbable collagen sponges soaked with recombinant human BMP-2 have been approved for clinical use in spinal fusion (INFUSE<sup>®</sup> bone graft; Medtronic, MN, USA). However, incorporation of BMP-2 into the carrier has numerous shortcomings including rapid clearance from the implant site and degradation by the proteolytic enzymes in the body [9]. The initial burst in BMP-2 has also made it difficult to maintain treatment efficiently throughout the period of tissue regeneration. Therefore, considerable efforts have been focused on the development of a controllable release system, which provides sustainable delivery during the period of healing and tissue regeneration without compromising its bioactive properties. Different types of carrier materials have been explored to increase the therapeutic efficacy by regulating the release of BMP-2 and its bioavailability [10]. For instance, incorporation of BMP-2 into biomimetic calcium phosphate coatings and hydroxyapatite-formed titanium surfaces [8,11], chemical crosslinking with scaffolds [12], and immobilization onto membrane surfaces such as chitosan nanofibers [10] are among several techniques investigated. Overall, all of the studied methods for combining BMP-2 with a carrier are mostly physical, the affinity of these delivery systems to the area of repair is limited, and they are inadequate for long-term control delivery [13].

Previous studies from our laboratory showed that enzymatically crosslinked BMP-2 to collagen scaffolds and hydrogels could control its release without diminishing its

biological activity [14,15]. Hence, the aim of this study is to examine the efficacy of such crosslinked BMP-2 hydrogels in rat cranial defect models. An ideal material for addressing craniofacial defect repair can conform to irregular shapes, rapidly solidify for provisional scaffolding, and assist tissue regeneration by active growth factors [7]. In our previous study, we demonstrated that transglutaminase (Tg)-Gel as a biocompatible and biodegradable natural polymer could be used as an injectable cell delivery system for wound healing applications [14]. Moreover, we substantiated that BMP-2 is bound to gelatin by site-specific crosslinking with Tg, where BMP-2 activity could be controlled through cellular digestive enzymes [15]. The use of such a gel as a bone graft proffers several advantages over the preformed solid scaffolds, which include the capacity to fill irregular defects, the flexibility in incorporating growth factors and/or cells, and the ease of placement on involved bone. Therefore, in this study, we evaluated the ability of an injectable collagen-based BMP-2-Tg-Gel and tested the composite gel graft for bone repair. The kinetics of BMP-2 activity regulated through collagenase digestion *in vitro* and autocrine/paracrine matrix metalloproteinase (MMP) action *in vivo* were also studied.

## Materials & methods

### Materials & reagents

BMP-2 of a stock concentration of 100 ng/ $\mu$ l was obtained from R&D Systems (MN, USA) and stored at  $-80^{\circ}\text{C}$  until use. Unless otherwise stated, all chemicals and reagents were purchased from Sigma-Aldrich (MO, USA).

Microbial Tg from *Streptomyces mobaraense* was obtained from Ajinomoto (Japan), and it was further purified with SP Sepharose Fast Flow beads (Sigma-Aldrich) as described [14,15]. Tg activity was titrated by the *o*-phthalaldehyde-hyde assay by using casein as a substrate [16], and protein concentration was tested by the Bradford method (Bio-Rad, CA, USA) [17] utilizing bovine serum albumin as a standard.

Gelatin Type B 225 Bloom (Sigma-Aldrich) was dissolved and autoclaved in distilled water to make 15% gelatin stock. 15% gelatin stock solution was then diluted with  $2\times$  phosphate-buffered saline (PBS) to make 7.5% gelatin and stored at  $4^{\circ}\text{C}$  until use. BMP-2 with a final concentration of 2000 ng/ml was mixed with gelatin, with or without 12 U/ml Tg crosslinking to create Tg-crosslinked gelatin gel with BMP-2 (BMP-2-Tg-Gel) and a BMP-2/gelatin blend, respectively.

### Cell culture

Mouse C2C12 myoblast cells (American Type Culture Collection [ATCC], VA, USA) and mouse NIH 3T3 fibroblast cells (ATCC) were cultured in high glucose DMEM (Mediatech, VA, USA) supplemented with 10% (v/v) fetal bovine serum (Lonza, MD, USA) and 1% (v/v) penicillin-streptomycin (Mediatech) at  $37^{\circ}\text{C}$  in a humidified atmosphere of 5%  $\text{CO}_2$ . The medium was changed every 2–3 days. Cells were subcultured when they reached 70% confluence using 0.25% trypsin and 0.02% EDTA solution.

### **C2C12 cell-based ALP activity assay**

BMP-2 activity was measured by using the method, as described in [15,18]. Briefly, gelatin or BMP-2/gelatin blend or BMP-2–Tg–Gel was applied to the transwell inserted in a 24-well cell culture plate seeded with  $5 \times 10^5$  C2C12 cells/well. Following the 48 h of coincubation at 37°C, the cell lysate was collected by washing the cells with PBS and homogenizing the cells with buffer solution (0.1% Triton X-100 in 1× PBS). After three freeze–thaw cycles, ALP activity was quantified by using *p*-NPP as a substrate (Pierce, IL, USA). The absorbance at 405 nm was measured by a multiplate reader (Molecular Devices, CA, USA) after 30 min of incubation at 37°C. The ALP activity was specified as an arbitrary unit of ALP absorbance. For tethered BMP-2, BMP-2 was released from Tg–Gel by adding 5 U/ml Type II microbial collagenase for 60 min (Worthington, NJ, USA) before the ALP activity test.

### **MMP gelatinolytic zymography assay**

MMP expression was assayed from cell culture conditional medium by gelatin zymography [15]. The cell-cultured medium was changed 24 h prior to the predetermined time points into a serum-free medium. The conditional medium was collected and stored at –20°C until assayed. Zymographic activities were revealed by 10% gelatin gel (Bio-Rad).

### **Autocrine reactivation of BMP-2**

Cells that were able to induce spontaneous BMP-2 activation were tested by coculturing C2C12 cells in gel tethered with BMP-2. C2C12 cells were detached using 0.25% trypsin and 0.02% EDTA to obtain a single-cell suspension, and then suspended in Tg–Gel or BMP-2–Tg–Gel at a cell density of  $3 \times 10^5$  cells/ml. 100 µl of the gel–cell mixture was pipetted into each well of a 48-well cell culture plate. The encapsulated cells were cultured for 2, 4, 6, 9 and 11 days at 37°C in a humidified atmosphere of 5% CO<sub>2</sub>. The intracellular ALP activity of the cell–gel constructs was quantified by the C2C12 cell-based ALP activity assay to procure the bioactivity of BMP-2.

### **Paracrine reactivation of BMP-2**

NIH 3T3 cells were used to assess the response of the MMPs to BMP-2–Tg–Gel. A total of  $4.5 \times 10^4$  NIH 3T3 cells/ml was seeded into each well of a 96-well cell culture plate; 200 µl complete medium was used on day 0 for cell attachment. Subsequently, 100 µl of the cultured medium was replaced by Tg-crosslinked 3% gel tethered with 6 ng/µl BMP-2. The cell culture medium of NIH 3T3 cells incubated with BMP-2–Tg–Gel was harvested daily and stored at –20°C until being further examined. The accumulated samples underwent a MMP gelatinolytic zymography assay and a C2C12 cell-based ALP activity assay to determine the presence of MMP and BMP-2 activity, respectively.

### ***In vitro* calvaria bone defect model**

Calvaria parietal bones were dissected from the heads of 4-day-old C57BL/6 mice. Throughout circular defects of 1.0 mm in diameter were created in the parietal bones using a skin puncher. The parietal bones were categorized into three groups: group I was empty (control), group II with insertion of Tg–Gel, and group III with insertion of 100 ng of

BMP-2 tethered with Tg–Gel (BMP-2–Tg–Gel). A total of 20  $\mu$ l of insertion was pipetted to fill the defect site accordingly. The induced bone defect models were cultured with the concave side faced down-ward in a six-well cell culture plate containing complete medium at 37°C in a humidified atmosphere of 5% CO<sub>2</sub> for 12 days. The cell culture medium was changed every 2 days.

### ***In vivo* cranial defect repair with BMP-2–Tg–Gel**

All animals used in this study followed the protocols that were approved by the Institutional Animal Care and Use Committees (IACUC) of the University of Southern California (CA, USA).

**Para-calvaria models**—Twenty-four 2-month-old Fischer-344 rats (National Cancer Institute, MD, USA) were randomly divided into four groups with different scaffold constructions. Group I consisted of gelatin only, group II consisted of Tg–Gel, group III comprised 1  $\mu$ g of BMP-2 mixed with 100  $\mu$ l of gelatin and group IV comprised 1  $\mu$ g of BMP-2 tethered with 100  $\mu$ l of Tg–Gel. Each animal was infused with 100  $\mu$ l of the prepared gel by using a G-27 needle subcutaneously injected over the parietal bone of the calvaria. The rats were euthanized 28 days after commencing the injections and the calvarial bones were removed for histological study. The removed calvarial bones were fixed, decalcified, and sectioned for hematoxylin and eosin (H&E) staining.

**Cranial defect models**—Twelve 2-month-old Fisher-344 rats were randomly divided into three groups: Tg–Gel (control); 200 ng of tethered BMP-2; and 500 ng of tethered BMP-2 mixture. The cranial defect was created by using a specially manufactured drill bit, which included a lip to restrict the depth of the circular cutting to create a circular opening of 5 mm in diameter in the skull of each rat. A total of 100  $\mu$ l of the prepared scaffold mixture was applied to the defect site by using a G-27 needle, and the skin incision was closed with a 4–0 Vicryl suture (Ethicon, NJ, USA). The rats were euthanized 14 days after commencing the injections, and the calvarial bones were removed for x-ray imaging and histological evaluation. The removed calvarial bones were fixed, decalcified and sectioned for H&E. Faxitron images were analyzed and calculated by ImageJ software (NIH, MD, USA).

### **Statistical analysis**

Data were expressed as mean  $\pm$  standard deviation for easier comparison. The Student's t-test was performed to examine the difference between the *in vivo* cranial defect models. Statistical significance was set at  $p < 0.05$  in all analyses.

## **Results**

### **Tethered BMP-2 activity in gel graft**

BMP-2 activity in a gel microenvironment, with or without Tg, was tested by using the C2C12 cell-based ALP activity assay as shown in Figure 1. Without Tg crosslinking, the 7.5% type B gelatin solidified within 60 min at room temperature, and subsequently dissolved in 2 h when incubated in culture medium at 37°C. Under these conditions, full BMP-2 activity was released (Figure 1, BMP-2/gelatin blend) within 2 h of incubation. By

contrast, when Tg was used to crosslink the gel with BMP-2, the gel solidified within 20 min at room temperature and remained in the gelation state for more than 48 h at 37°C. Less than 10% of the BMP-2 activity (Figure 1, BMP-2–Tg–Gel) was detected, indicating that there was little to no BMP-2 leakage. However, when collagenase was used to digest the gelatin, the full tethered BMP-2 activity was released (Figure 1, released BMP-2), which approximately equalled the level released by the positive control (Figure 1, BMP-2).

### **Tethered BMP-2 reactivation by autocrine MMP**

C2C12 cells were selected to study BMP-2 reactivation via autocrine fashion based on the following facts: C2C12 cells are BMP-2 reporter cells and they are able to express MMP-2 when grown in a 3D gel environment [15]. Moreover, C2C12 is a premyoblast cell whose ALP expression is close to baseline levels without BMP stimulation. However, the question of whether autocrine MMP expression by C2C12 can activate tethered BMP-2 remained unclear. In this study, C2C12 cells were embedded in BMP-2–Tg–Gel and were allowed to culture for a total of 11 days. The resulting ALP activity is shown in Figure 2. The encapsulated cells in the BMP-2–Tg–Gel microenvironment demonstrated higher BMP-2 activity than those cells loaded in Tg–Gel (Figure 2A). In addition, a gradual increase in MMP-2 along with an increase in ALP activity over time was observed (Figure 2A & 2B). This suggested that the cellular MMP activity may serve as a cell-controllable switch to turn on tethered BMP-2 in a Tg–Gel system. The cells in the BMP-2–Tg–Gel tended to aggregate and further substantiate cell differentiation from a single rounded cell to an extended branch network (Figure 2C). However, more rounded cells and relatively less elongated cells were found in the Tg–Gel without BMP-2.

### **Tethered BMP-2 paracrine activation**

NIH 3T3 cells were chosen to test if neighboring cells such as fibroblasts would reactivate tethered BMP-2 due to their ability to release MMPs in response to their surrounding environment [19,20]. As shown in Figure 3, the NIH 3T3 cells produced MMP-2 and MMP-9 when they were incubated with the BMP-2–Tg–Gel (Figure 3A). Moreover, the tethered BMP-2 releasing rate (as a function of ALP activity) increased with the NIH 3T3 cells incubation time from day 1 to 4. The BMP-2 activity declined on the fifth day, which might be due to degradation or digestion of BMP-2 over a prolonged culture period. Furthermore, the BMP-2–Tg–Gel group exhibited higher ALP activity than the Tg–Gel group indicating that surrounding cells might be involved in aiding the reactivation of tethered BMP-2 (Figure 3B). Scrutinizing these data and observations, the tethered BMP-2 in the bone graft might be activated through the environmental cells in a paracrine fashion.

### **Ex vivo repair model**

The phase contrast images of the induced 1.0-mm murine calvaria defects treated with either vehicle (control) or Tg–Gel, with or without tethered BMP-2 for 6 and 12 days, are shown in Figure 4. The defects without any gel application remained wide open on days 6 and 12, with few cells growing toward the central hole at day 12 (Figure 4A–D). However, improved results were obtained when using Tg–Gel as a scaffold (Figure 4E–H), with some of the cells at the edge of the defect starting to grow inward. The cells reached the center of the defect by day 12. Importantly, a striking contrast was observed in the defect treated

with BMP-2–Tg–Gel. At day 6, the cells grew from the edge toward the center uniformly. Moreover, the cells traveled significantly further to the center of the defect than the Tg–Gel group, where half of the defects were covered with cells and soft tissues. By day 12, the cells and the dense extracellular matrix shielded the entire defect (Figure 4I–L).

### **Bone formation in the cranial overlay model**

Animals were euthanized 28 days after subcutaneous injection of 100  $\mu$ l of various gel preparations over the calvaria. A semiquantitative histological score scale was used to evaluate new bone formation and gel contour, as shown in Figure 5. Gelatin without Tg crosslinking completely dissolved at the injection site after 28 days, and no new bone formation was visualized regardless of the concentration of BMP-2, as depicted in Figure 5 (group I and III), indicating that rapid diffusion of BMP-2 and degradation of scaffold failed to induce bone formation. When gelatin was crosslinked with Tg (Figure 5, group II), the gel contour on the top of the calvaria was still well preserved after 4 weeks. Furthermore, infiltration of fibroblasts, inflammation cells and neovessel invasion were observed. A small area of new bone was formed inside the gel graft adjacent to the bony calvaria, indicating Tg–Gel is an osteoconductive scaffold. In group IV, BMP-2–Tg–Gel induced new bone formation within the contour of the gel graft and approximately 80% of the gel graft was replaced by mature bone after 4 weeks (Figure 5, group IV). In addition, blood vessels were found evenly scattered throughout the new bone area and the remaining remodeled gel edge was lined up with the osteoblasts.

### **Bone repair in the cranial defect model**

Finally, bony defect repairs by injectable bone grafts were tested in rat cranial defect models. 100  $\mu$ l of the injectable bone graft was applied by syringe delivery to the cranial bone defect area. The gel bone graft covered the defect without diffusion or migration, possibly owing to the additional crosslinking reaction between the gel and collagenous tissues at the defect site. In Figure 6, x-ray imaging revealed that there was little bone formation in the control group (Tg–Gel without BMP-2) 14 days after bone grafting (Figure 6A). Furthermore, obvious bone formation was observed in the tethered BMP-2 test arms (Figure 6A). ImageJ demonstrated that the area of new bone formation depended on the concentration of the tethered BMP-2 (Figure 6B, 0 vs 200 ng,  $p < 0.05$ ; 200 vs 500 ng,  $p < 0.01$ ). H&E examination (as shown in Figure 7) revealed new bone formation within the defect with the greatest observed in the 500 ng BMP-2–Tg–Gel group and lowest in the control group. The area of new bone formation in the 200 ng BMP-2–Tg–Gel group (Figure 7B & 7E) was greater than those in the Tg–Gel group (Figure 7A & 7D), yet smaller than the area in the 500 ng BMP-2–Tg–Gel group (Figure 7C & 7F). Moreover, new bone area was not only observed adjacent to the calvarial bone, but also in the center of the Tg–Gel. There was little bone formation visualized in the control group (Figure 7A & 7D), but its position near the edge of the defect reveals that Tg–Gel is an osteoconductive scaffold.

## **Discussion**

BMP-2 is essential for initiating fracture healing [21], as well as for osteoinduction of dural pericytes in calvarial defect models [22]. However, obstacles such as high cost,

short retention time, and side effects caused by the large amount of BMP-2 required to promote osteogenesis have limited its widespread use. It has been demonstrated that a prolonged presence of BMPs within the defect site is desirable for bone regeneration [23]. BMP-2 released from gelatin alone or other ceramic scaffolds produces a large initial burst, resulting in an imbalanced release of BMP-2 [12]. In this study, we introduced Tg–Gel, which regulated the release of BMP-2 and promoted bone reconstruction in the induced cranial defect models. We also demonstrated that BMP-2–Tg–Gel could be administered in a semiliquid form to fit any defect and solidified to serve as a tissue regeneration and remodeling scaffold.

Gelatin is able to be readily transform from solid phase to liquid phase or *vice versa* repeatedly. The flexible thermal transformative property of the gel allows it to be easily injected into defects of any size and shape. However, the mechanical property of gelatin itself is relatively weak. Thus, it is important to develop a material that has a higher solidification rate, is thermally and mechanically stable under physiological conditions, and has a controllable degradation rate *in vivo* [5,24]. In our study, the 7.5% gelatin took approximately 1 h to solidify at room temperature and 2 h for it to return to liquid state at 37°C. By using Tg as an enzymatic crosslinking agent, we were able to covalently bind the gel's  $\epsilon$ -amino group of lysine and  $\gamma$ -carboxamide group of glutamine to produce a biocompatible and physiologically robust cellular scaffold [25–27]. Tg took approximately 30 min to crosslink with the gel, which was considerably faster than the gelatin without any crosslinking. Once the crosslinked gel solidified, the gel remained intact without degradation for the entire 4 weeks of our *in vivo* test period and the shape of the gel was well preserved. The demonstrated characteristic of the Tg–Gel as a scaffold is crucial in supporting the defect site until the bone is fully restored. In addition, the injectable Tg–Gel reduces the need for handling and minimizes the invasive procedures needed as opposed to conventional autograft or allograft implantations.

The effects of BMP-2 are concentration dependent. Due to the rapid local clearance and short biological half-life of BMP-2, its clinical application is not always cost effective [28]. High dose application of BMP-2 has been used to address this problem; yet, this invariably leads to undesirable effects. Previous studies showed that high dosage or continuous injection of BMP-2 could exacerbate the quality of the bone formation and its mechanical properties while inducing abnormal structure [29]. Moreover, adverse clinical effects such as seromas, cyst-like bone formation, significant soft tissue swelling, stimulation of bone resorption, heterotopic and excessive bone formation, and nerve cell reaction in un intended areas have also been identified [15,29–31]. Therefore, several groups [8,28,30], including our laboratory, have devoted extensive efforts to improve the delivery of BMP-2. Protein conjugation is one of the many approaches to control the activity of proteins and prolong their half-life. Fontana *et al.* demonstrated that Tg could be used to protect the cleavage site from proteolysis through covalent linkage between peptides [32]. In some proteins, the sites of Tg reaction are also the sites of proteolysis, and thus, the bonds formed by the Tg are not cleavable or digestible by any known enzymes [32]. This has suggested that a reaction method could be incorporated into our system to prevent proteolysis when the sites are occupied. Previously, Sato *et al.* bound alkylamine derivatives of polyethylene glycol to



IL-2 and discovered that this extended the half-life of IL-2 to approximately four-times the half-life of the unbound IL-2 [33].

We took advantage of the fact that BMP-2 has endogenous reactive sites for Tg to bind to, allowing it to be tethered onto a suitable reactive scaffold such as gelatin [15,34]. In our previous study [15], we showed that the osteoinductive potential of high BMP-2 doses could be regulated by tethering it with a degradable matrix through enzymatic crosslinking. The tethering of BMP-2 to the Tg–Gel not only prevented its initial burst release, but also allowed the BMP-2 bioactivity to be controlled by cell–material interaction. The amount of initial burst of BMP-2 detected in the BMP-2–Tg–Gel (10% of the total amount of BMP-2) was insignificant when compared with the BMP-2/gelatin blend, where gelatin alone as the BMP-2 carrier exhibited an initial burst release of more than 80% of the total amount of BMP-2 [12]. The trivial initial burst observed in our study might be due to the diffusion of free-state BMP-2 from the Tg–Gel right after injection. The small amount of untethered BMP-2 may be crucial in triggering the repair cascade at the beginning of the healing state, but the optimal dosage requires further examination. The majority of the BMP-2 tethered to the Tg remained in its latent state until it was activated by proteinases secreted from the cells. It is worth noting that the dosage of BMP-2 used in this animal study is less than the required amount for similar animal models, where 5–40 µg of BMP-2 is needed for effective bridging of the defect [29,35]. However, we substantiated that less than 1 µg of BMP-2 was sufficient to promote bone repair in our study.

This study demonstrated that the Tg–Gel itself was an osteoconductive graft, and it enhanced bone formation in the rat calvaria overlay and the cranial defect models when tethered with BMP-2. The Tg–Gel crosslinked with BMP-2 prolonged the persistence of the BMP-2 locally to allow the osteoprogenitor cells to migrate to the target site and differentiate into osteoblasts. With the aid of the Tg–Gel, the de-activated BMP-2 was slowly released by the proteinase action through both autocrine and paracrine pathways at the repair site.

## Conclusion

It has become evident that an adjuvant material for repairing genetic or accidental bone defects needs to mimic the physiological environment to support and control the release of the growth factors to amplify the regenerative capacity. Nonetheless, there are two key aspects that must be taken into consideration for fabricating a practical physiological scaffold: chemical signals, such as growth factors and cytokines, which are crucial for tissue repair; and mechanosignals, such as stress and strain, which are important adjuvants for material design. We believe that we have begun to successfully address some of these important parameters.

## Future perspective

BMP-2 has been known to induce bone formation. However, BMP-2 without tethering with any scaffold produces a large initial burst which has limited its widespread use in healing bone defects. Moreover, the high concentrations of BMP at the defect sites cause adverse

effects. To circumvent such limited functionality or vitality, BMP-2 can be crosslinked with Tg–Gel. This allows for a controllable release of BMP-2, avoids the initial burst and prolongs the half-life of BMP-2. Although this chemical signal (BMP-2) demonstrated bone formation, mechanical signals play a vital role in influencing cell behavior. Therefore, further evaluation of the material properties including stiffness, pore size, and degradation rate and the synergetic effects of mechanical and chemical signals are warranted for optimally mimicking the physiological microenvironment of the target site.

## Financial & competing interests disclosure

This project was supported by SC CTSI (NIHNCRR/NCATS) through grant UL1RR031986. The authors have no other relevant affiliations or financial involvement with any organization or entity with a financial interest in or financial conflict with the subject matter or materials discussed in the manuscript apart from those disclosed.

No writing assistance was utilized in the production of this manuscript.

## References

Papers of special note have been highlighted as: \*\* of considerable interest

- Burchardt H, Busbee GA 3rd, Enneking WF. Repair of experimental autologous grafts of cortical bone. *J. Bone Joint Surg. Am* 57(6), 814–819 (1975). [PubMed: 1099104]
- Graham JM, Phelps PD, Michaels L. Congenital malformations of the ear and cochlear implantation in children: review and temporal bone report of common cavity. *J. Laryngol. Otol* 114, 1–14 (1999).
- Szpalski C, Barr J, Wetterau M, Saadeh PB, Warren SM. Cranial bone defects: current and future strategies. *Neurosurg. Focus* 29(6), e8 (2010).
- Ginebra MP, Canal C, Espanol M, Pastorino D, Montufar EB. Calcium phosphate cements as drug delivery materials. *Adv. Drug Deliv. Rev* 64(12), 1090–1110 (2012). [PubMed: 22310160]
- Ambrosio L, Guarino V, Sanginario V et al. Injectable calcium-phosphate-based composites for skeletal bone treatments. *Biomed. Mater* 7(2), 024113 (2012). [PubMed: 22456083]
- Kurashina K, Kurita H, Hirano M, Kotani A, Klein C, De Groot K. *In vivo* study of calcium phosphate cements: implantation of an  $\alpha$ -tricalcium phosphate/dicalcium phosphate dibasic/tetracalcium phosphate monoxide cement paste. *Biomaterials* 18(7), 539–543 (1997). [PubMed: 9105593]
- Dumas JE, BrownBaer PB, Prieto EM et al. Injectable reactive biocomposites for bone healing in critical-size rabbit calvarial defects. *Biomed. Mater* 7(2), 024112 (2012). [PubMed: 22456057]
- Bae SE, Choi J, Joung YK, Park K, Han DK. Controlled release of bone morphogenetic protein (BMP)-2 from nanocomplex incorporated on hydroxyapatite-formed titanium surface. *J. Control. Release* 160(3), 676–684 (2012). [PubMed: 22543042]
- McKay WF, Peckham SM, Badura JM. A comprehensive clinical review of recombinant human bone morphogenetic protein-2 (INFUSE® Bone Graft). *Int. Orthop* 31(6), 729–734 (2007). [PubMed: 17639384]
- Park YJ, Kim KH, Lee JY et al. Immobilization of bone morphogenetic protein-2 on a nanofibrous chitosan membrane for enhanced guided bone regeneration. *Biotechnol. Appl. Biochem* 43(1), 17–24 (2006). [PubMed: 15910285]
- Liu Y, Huse RO, de Groot K, Buser D, Hunziker EB. Delivery mode and efficacy of BMP-2 in association with implants. *J. Dent. Res* 86(1), 84–89 (2007). [PubMed: 17189469]
- Liu Y, Lu Y, Tian X et al. Segmental bone regeneration using an rhBMP-2-loaded gelatin/nanohydroxyapatite/fibrin scaffold in a rabbit model. *Biomaterials* 30(31), 6276–6285 (2009). [PubMed: 19683811]
- Zhang Q, He QF, Zhang TH, Yu XL, Liu Q, Deng FL. Improvement in the delivery system of bone morphogenetic protein-2: a new approach to promote bone formation. *Biomed. Mater* 7(4), 045002 (2012). [PubMed: 22556155]

14. Kuwahara K, Yang Z, Slack GC, Nimni ME, Han B. Cell delivery using an injectable and adhesive transglutaminase–gelatin gel. *Tissue Eng. Part C Methods* 16(4), 609–618 (2009). ■■ First to demonstrate that transglutaminase-crosslinked gelatin can be administered as an injectable carrier for cell delivery.
15. Kuwahara K, Fang JY, Yang Z, Han B. Enzymatic crosslinking and degradation of gelatin as a switch for bone morphogenetic protein-2 activity. *Tissue Eng. Part A* 17(23–24), 2955–2964 (2011). [PubMed: 21882896] ■■ First to discover that BMP-2 can be deactivated when it binds to transglutaminase-crosslinked gelatin gel and it can be reactivated via collagenase or tissue-derived matrix metalloproteinases.
16. Dinnella C, Gargaro MT, Rossano R, Monteleone E. Spectrophotometric assay using *o*-phthaldialdehyde for the determination of transglutaminase activity on casein. *Food Chem.* 78(3), 363–368 (2002).
17. Bradford MM. A rapid and sensitive method for the quantitation of microgram quantities of protein utilizing the principle of protein-dye binding. *Anal. Biochem* 72(1), 248–254 (1976). [PubMed: 942051]
18. Han B, Tang B, Nimni ME. Quantitative and sensitive *in vitro* assay for osteoinductive activity of demineralized bone matrix. *J. Orthop. Res* 21(4), 648–654 (2003). [PubMed: 12798064]
19. Maxová H, Bacakova L, Lisá V et al. Production of proteolytic enzymes in mast cells, fibroblasts, vascular smooth muscle and endothelial cells cultivated under normoxic or hypoxic conditions. *Phys. Res* 59, 711–719 (2010).
20. Chau D, Collighan RJ, Verderio EA, Addy VL, Griffin M. The cellular response to transglutaminase-crosslinked collagen. *Biomaterials* 26(33), 6518–6529 (2005). [PubMed: 15927250]
21. Tsuji K, Bandyopadhyay A, Harfe BD et al. BMP2 activity, although dispensable for bone formation, is required for the initiation of fracture healing. *Nat. Genet* 38(12), 1424–1429 (2006). [PubMed: 17099713]
22. Takagi K, Urist MR. The reaction of the dura to bone morphogenetic protein (BMP) in repair of skull defects. *Ann. Surg* 196(1), 100–109 (1982). [PubMed: 7092346] ■■ First to successfully demonstrate that implanted BMP induces skull trephine defects during bone regeneration.
23. Schmoekel H, Schense JC, Weber FE et al. Bone healing in the rat and dog with nonglycosylated BMP-2 demonstrating low solubility in fibrin matrices. *J. Orthop. Res* 22(2), 376–381 (2004). [PubMed: 15013099]
24. Young S, Wong M, Tabata Y, Mikos AG. Gelatin as a delivery vehicle for the controlled release of bioactive molecules. *J. Control. Release* 109(1), 256–274 (2005). [PubMed: 16266768]
25. Yung CW, Wu LQ, Tullman JA, Payne GF, Bentley WE, Barbari TA. Transglutaminase crosslinked gelatin as a tissue engineering scaffold. *J. Biomed. Mater. Res. A* 83(4), 1039–1046 (2007). [PubMed: 17584898]
26. Chen T, Small DA, McDermott MK, Bentley WE, Payne GF. Enzymatic methods for *in situ* cell entrapment and cell release. *Biomacromolecules* 4(6), 1558–1563 (2003). [PubMed: 14606880]
27. Folk JE. Mechanism and basis for specificity of transglutaminase-catalyzed  $\epsilon$ -( $\gamma$ -glutamyl) lysine bond formation. *Adv. Enzymol. Relat. Areas Mol. Biol* 54, 1–56 (1983). [PubMed: 6133417]
28. Lee JW, Lee S, Lee SH et al. Improved spinal fusion efficacy by long-term delivery of bone morphogenetic protein-2 in a rabbit model. *Acta Orthop.* 82(6), 756–760 (2011). [PubMed: 22066556]
29. Zara JN, Siu RK, Zhang X et al. High doses of bone morphogenetic protein 2 induce structurally abnormal bone and inflammation *in vivo*. *Tissue Eng. Part A* 17(9–10), 1389–1399 (2011). [PubMed: 21247344] ■■ First to determine the dose-dependent effects of BMP-2 by incorporating multiple BMP-2 doses into a rat femoral segmental defect model and minimally traumatic rat femoral model.
30. Zhou H, Qian J, Wang J et al. Enhanced bioactivity of bone morphogenetic protein-2 with low dose of 2-*N*, 6-*O*-sulfated chitosan *in vitro* and *in vivo*. *Biomaterials* 30(9), 1715–1724 (2009). [PubMed: 19131102]

31. Kinsella CR, Bykowski MR, Lin AY et al. BMP-2-mediated regeneration of large-scale cranial defects in the canine: an examination of different carriers. *Plast. Reconstr. Surg* 127(5), 1865–1873 (2011). [PubMed: 21532416]
32. Fontana A, Spolaore B, Mero A, Veronese FM. Site-specific modification and PEGylation of pharmaceutical proteins mediated by transglutaminase. *Adv. Drug Deliv. Rev* 60(1), 13–28 (2008). [PubMed: 17916398] ■■ First to demonstrate that transglutaminase can be used to protect the cleavage site from proteolysis through covalent linkage between peptides.
33. Sato H Enzymatic procedure for site-specific pegylation of proteins. *Adv. Drug Deliv. Rev* 54(4), 487–504 (2002). [PubMed: 12052711] ■■ First to bind alkylamine derivatives of polyethylene glycol to IL-2 and discover that the binding can extend the half-life of IL-2 to approximately four-times the half-life of unbound IL-2.
34. Ito A, Mase A, Takizawa Y et al. Transglutaminase-mediated gelatin matrices incorporating cell adhesion factors as a biomaterial for tissue engineering. *J. Biosci. Bioeng* 95(2), 196–199 (2003). [PubMed: 16233392]
35. Yasko AW, Lane JM, Fellingner EJ, Rosen V, Wozney JM, Wang EA. The healing of segmental bone defects, induced by recombinant human bone morphogenetic protein (rhBMP-2). A radiographic, histological, and biomechanical study in rats. *J. Bone Joint Surg. Am* 74(5), 659 (1992). [PubMed: 1378056]

## Executive summary

### Controlling BMP-2 activity

- Controlling BMP-2 activity was critical for bone reconstruction.
- This study demonstrated that BMP-2 tethered to a gelatin gel by using transglutaminase (Tg) as a crosslinking agent controlled its activity and prolonged its half-life.
- The tethered BMP-2 could be reactivated through autocrine and paracrine pathways.
- The reactivated BMP-2 was measured by the presence of matrix metalloproteinase proteins.

### *Bone formation in vitro & in vivo*

- Tg-crosslinked gelatin gel (Tg-Gel) with its osteoconductive properties was capable of promoting bone formation.
- Tg-Gel with BMP-2 (BMP-2-Tg-Gel) induced greater bone formation throughout the experiment compared with BMP-2 and Tg-Gel alone.
- Less than 1  $\mu\text{g}$  of BMP-2 was sufficient to induce new bone formation in rat animal models.

### Injectable drug delivery system for bone defects

- BMP-2-Tg-Gel as an injectable drug delivery system may provide minimally invasive surgical procedures in treating irregularly shaped bone defects (e.g., cranial defects).
- The BMP-2-Tg-Gel introduced in this study demonstrated promising results and may be an alternative approach for the treatment of critical bone defects.

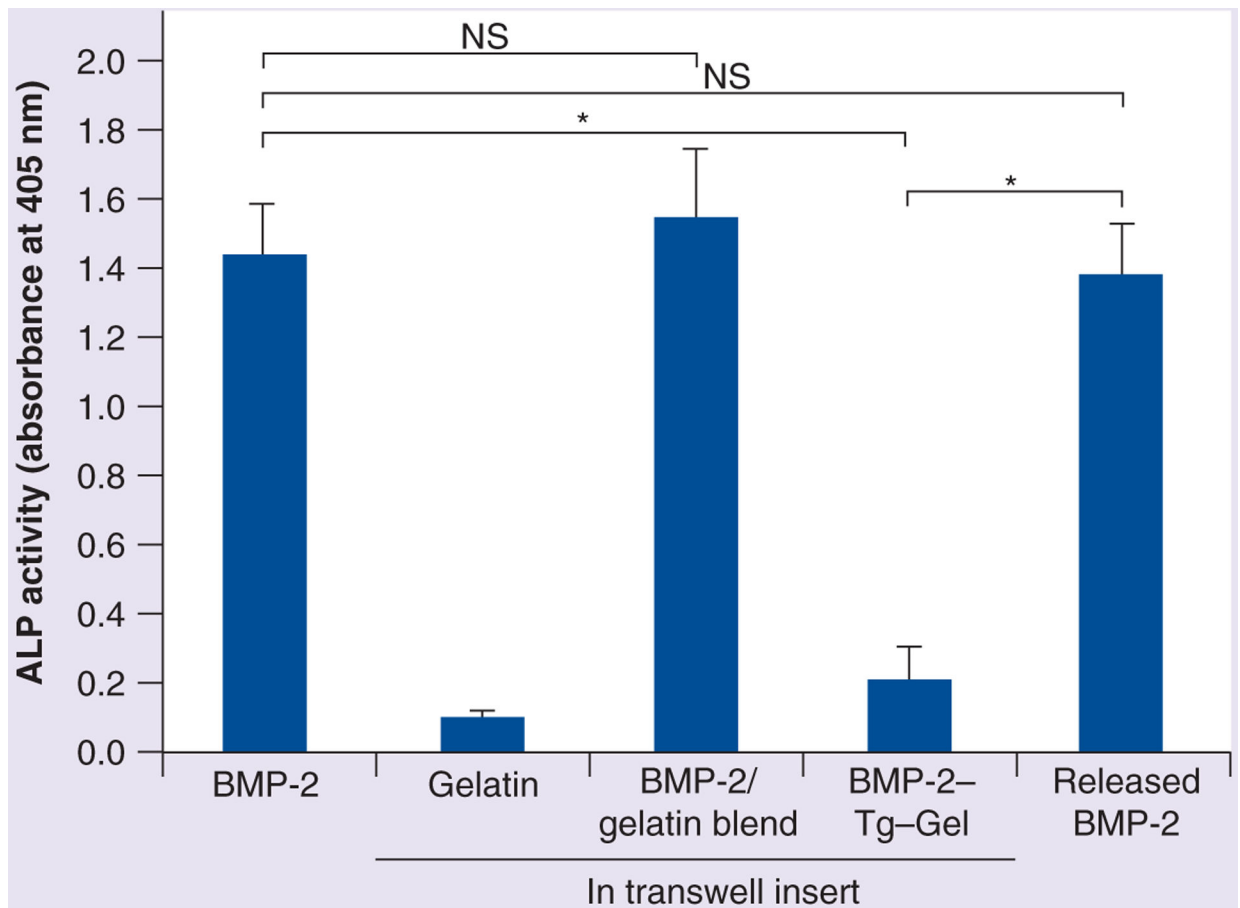


**Figure 1. Induced ALP activity associated with various gel and/or BMP-2 preparations.** BMP-2 served as a positive control and gelatin served as a negative control for ALP activity induced by BMP-2. BMP-2/gelatin blend denotes BMP-2 mixed with the gel but without any Tg crosslinking, and BMP-2-Tg-Gel indicates BMP-2 tethered with gel crosslinked with Tg where BMP-2 remained in a bound state. Released BMP-2 represents BMP-2 activity released by bacterial collagenase from BMP-2-Tg-Gel (n = 4). Data are expressed as mean  $\pm$  standard deviation.

\*p < 0.01.

BMP-2-Tg-Gel: Transglutaminase-crosslinked gelatin gel with BMP-2; NS: Not significant; Tg: Transglutaminase.

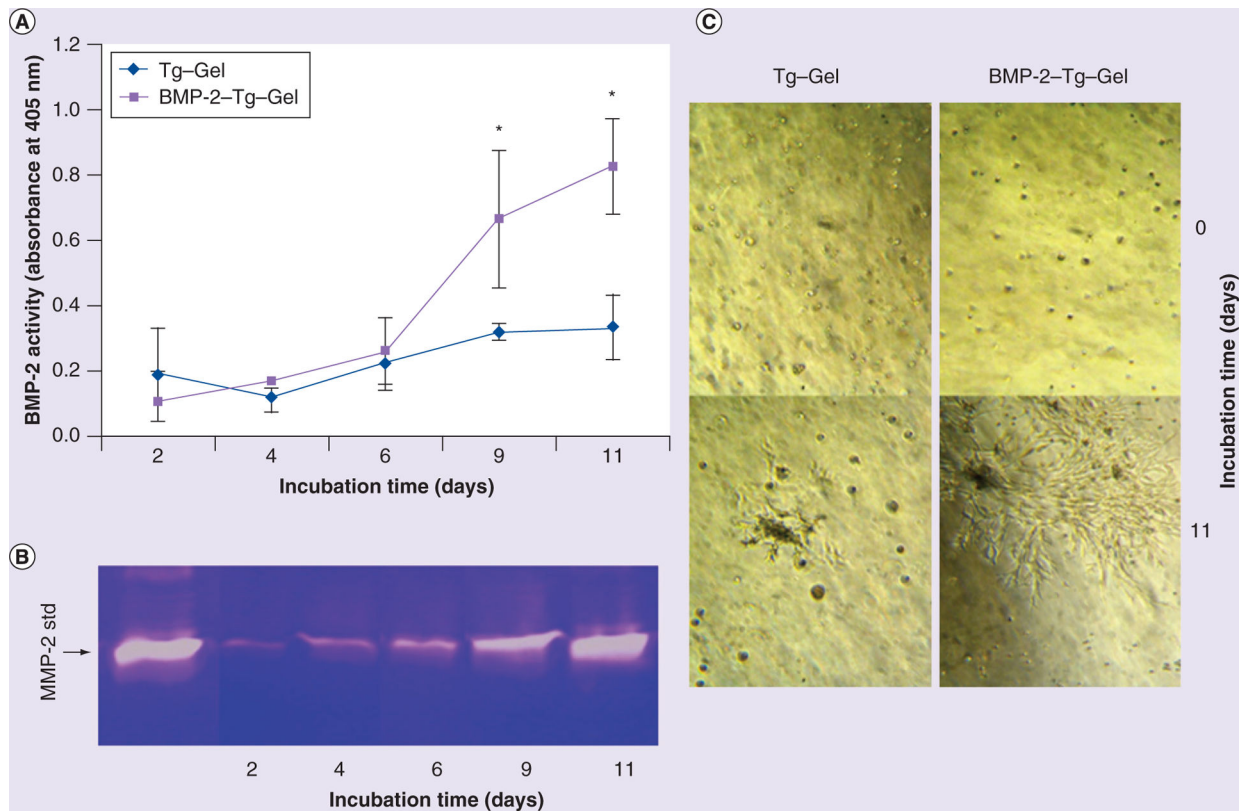


**Figure 2. Tethered BMP-2 reactivation as a result of autocrine MMP-2 secretion by C2C12 cells.** (A) Reactivated BMP-2 activity from BMP-2-Tg-Gel by a C2C12-derived proteinase. Cell membrane associated with ALP activity was tested by harvesting the cells at predetermined time periods (days 2, 4, 6, 9 and 11; n = 4). Data are expressed as mean  $\pm$  standard deviation. (B) Gelatin zymograph showed native MMP-2 secretion from C2C12 cells grown in gel for 2, 4, 6, 9 and 11 days. (C) Cell morphology with or without tethered BMP-2 gel on days 0 and 11.

\*p < 0.01.

BMP-2-Tg-Gel: Transglutaminase-crosslinked gelatin gel with BMP-2; std: Standard; Tg-Gel: Transglutaminase-crosslinked gelatin gel.

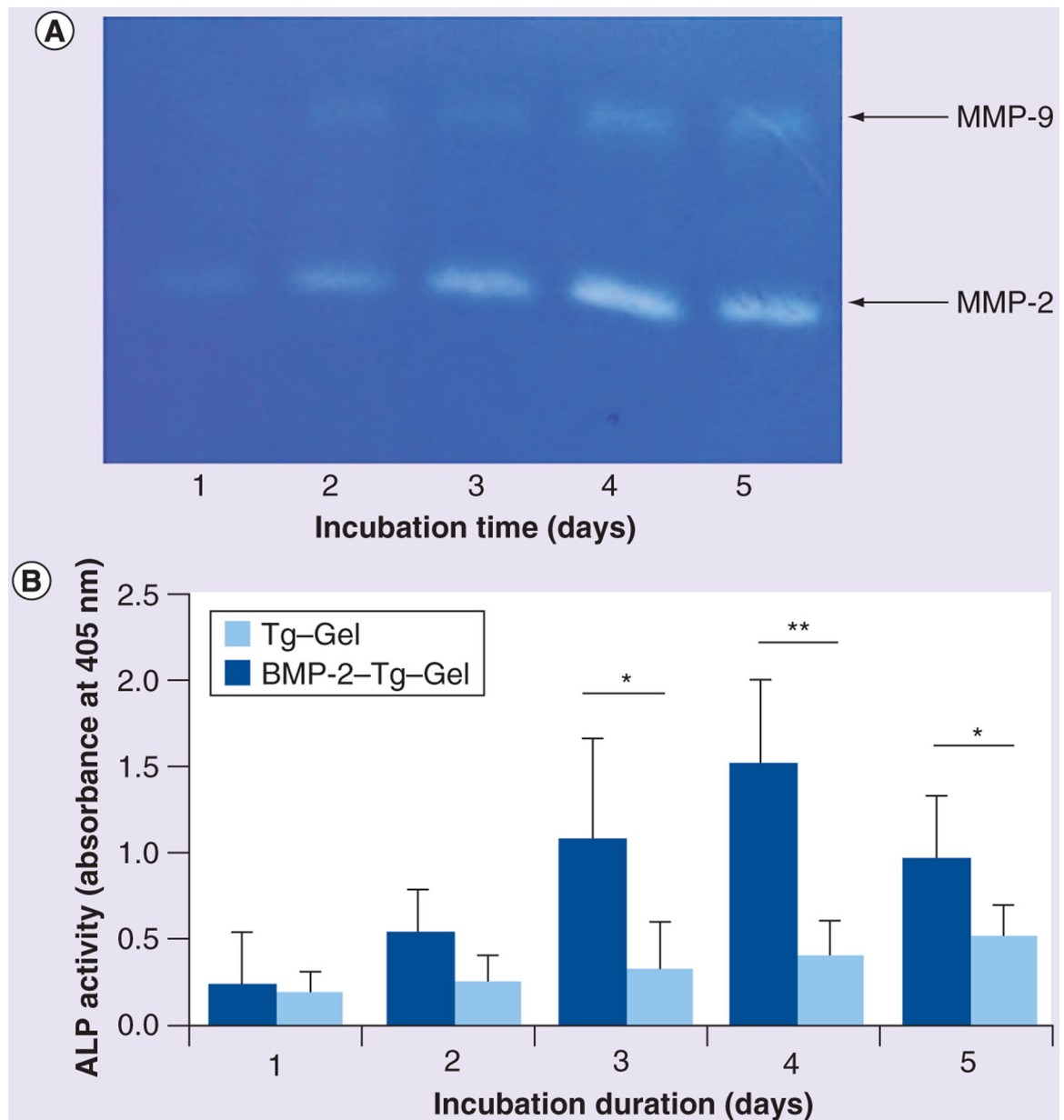


**Figure 3. Reactivation of the tethered BMP-2 in transglutaminase-crosslinked gelatin gel by NIH 3T3 cells.**

(A) Gelatin zymograph showed native MMP-2 and MMP-9 secretion from NIH 3T3 cells for days 1–5. MMP-2 and MMP-9 have the molecular weight of 72 and 92 kDa, respectively. (B) ALP activity was tested by harvesting the cell culture medium of NIH 3T3 that was incubated with BMP-2–Tg–Gel on days 1–5. C2C12 cells were exposed to each medium for 48 h at 37°C before the ALP activity assay (n = 4). Data are expressed as mean ± standard deviation.

\*p < 0.05; \*\*p < 0.01.

BMP-2–Tg–Gel: Transglutaminase-crosslinked gelatin gel with BMP-2; Tg–Gel: Transglutaminase-crosslinked gelatin gel.



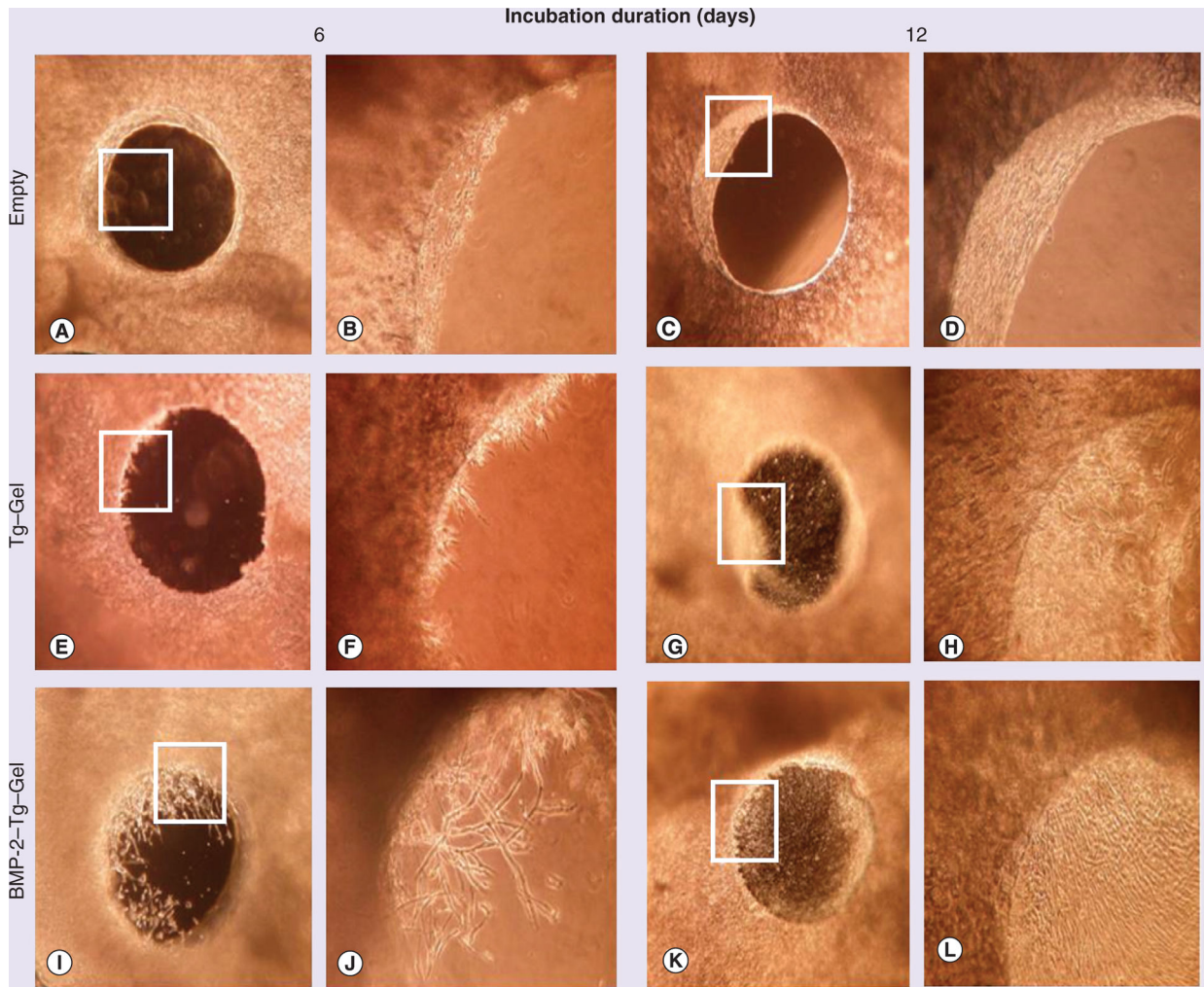


**Figure 4. Bone repair through gel constructs in calvaria bone organ culture model.** Phase contrast images of 1.0-mm defects on days 6 and 12 of various treatments. Empty served as a negative control without any gel. A total of 20  $\mu$ l of assigned gel construct was applied to each calvaria defect placed at the bottom of a 24-well cell culture plate accordingly. Images (A, C, E, G, I & K) were visualized at a magnification of 40 $\times$ , and images (B, D, F, H, J & L) were pictured at a magnification of 100 $\times$  using an inverted light microscope (Nikon, Japan), and are higher magnification images of the boxed sections in (A, C, E, G, I & K), respectively. BMP-2-Tg-Gel: Transglutaminase-crosslinked gelatin gel with BMP-2; Tg-Gel: Transglutaminase-crosslinked gelatin gel.

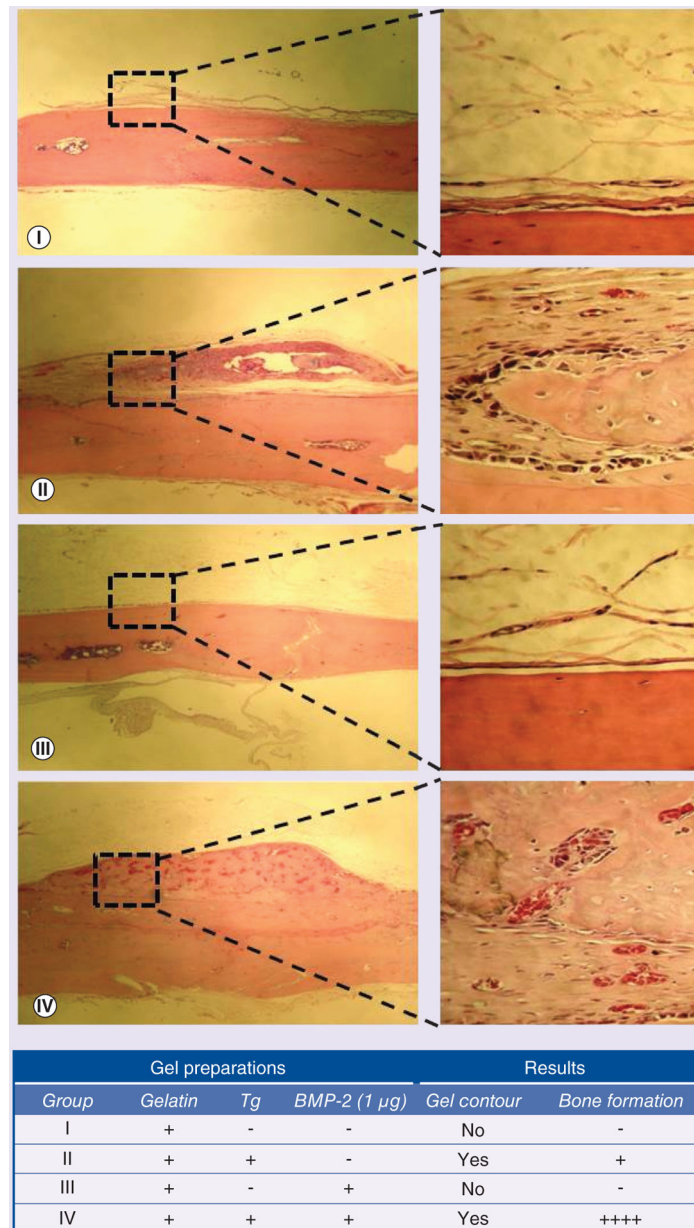


**Figure 5. Comparison of bone formation with different gel constructs in the cranial overlay models.**

After 28 days of subcutaneous injection, explants underwent histology evaluation.

Hematoxylin and eosin staining was performed for group I (gelatin), group II (transglutaminase-crosslinked gelatin gel), group III (gelatin/BMP-2 blend) and group IV (transglutaminase-crosslinked gelatin gel with BMP-2). The right panels (400 $\times$ ) demonstrate higher magnification images of the boxed sections in the left panels (40 $\times$ ). These were taken to better visualize the new tissue formation. The higher magnification images of group II and IV show tissue ingrowth into the scaffold, while group I and III demonstrated no bone regeneration.

-: No bone; +: 1–25% bone; +++++: 75–100% bone; Tg: Transglutaminase.

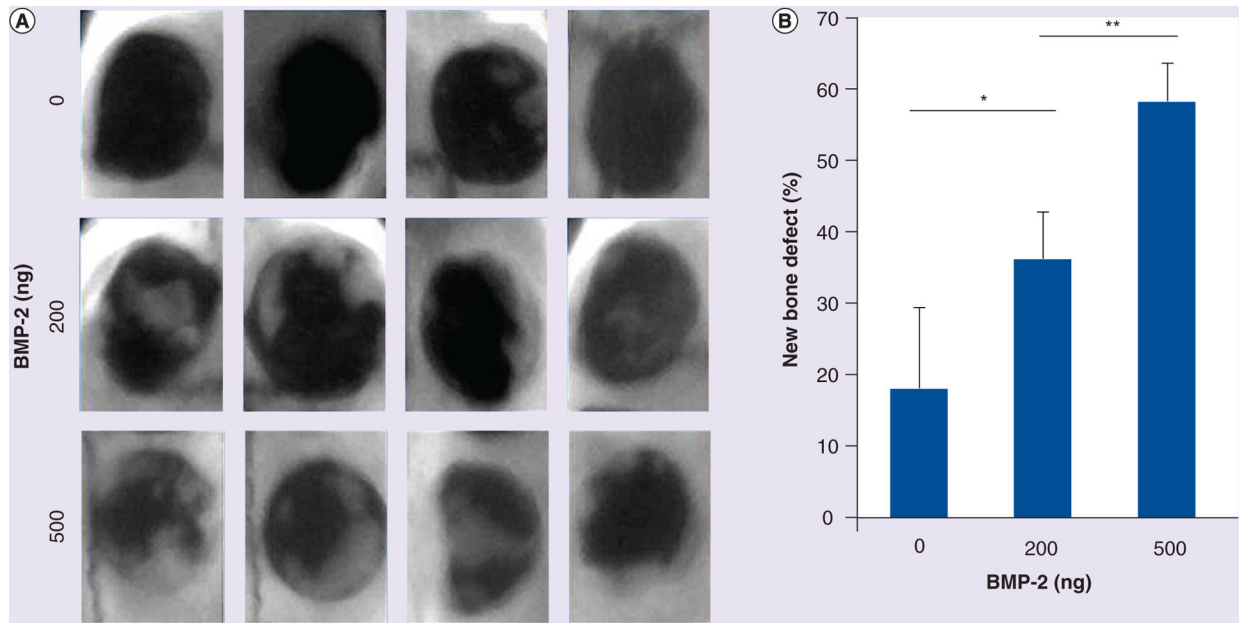


**Figure 6. Bone repair in cranial defect models.**

After 14 days of subcutaneous injection, x-ray images of calvaria bone repair were captured for the 12 rat models. (A) Faxitron images of bone repair at the defect site 14 days after the administration of tethered BMP-2 (0, 200 and 500 ng). (B) New bone area was analyzed and calculated using ImageJ software (NIH, MD, USA). Data are expressed as mean  $\pm$  standard deviation.

\*p < 0.05; \*\*p < 0.01.

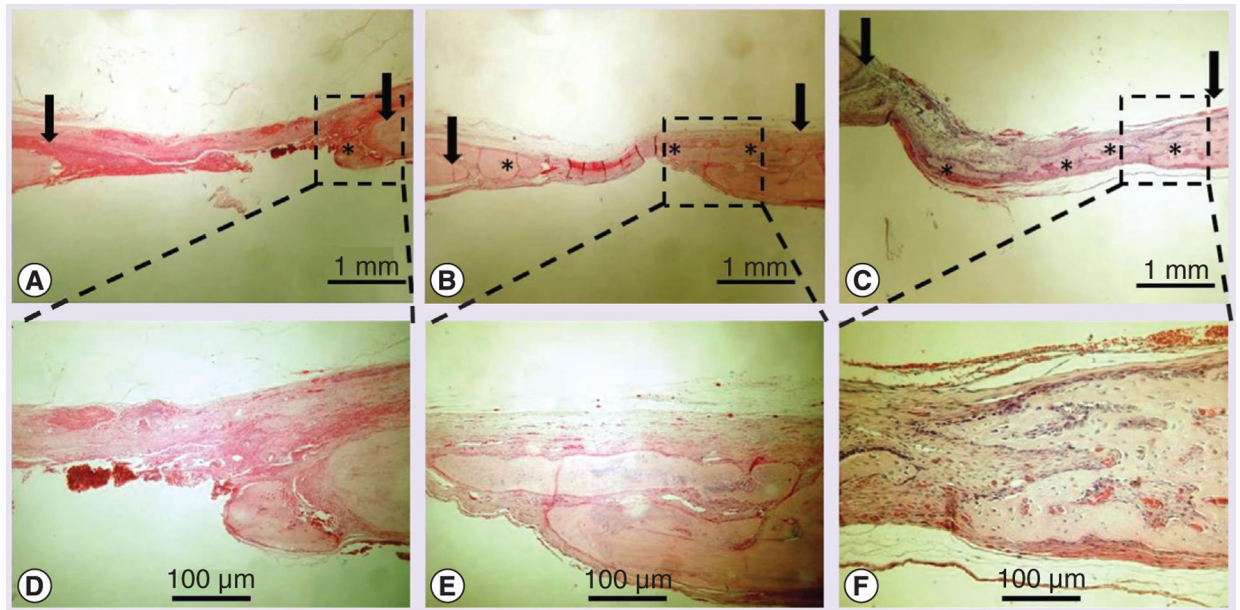


**Figure 7. Osteoinductivity of transglutaminase-crosslinked gelatin gel with BMP-2 *in vivo* cranial defect models.**

A total of 14 days after grafting, explants underwent histology evaluation (arrow indicates bone defect edge, \* indicates new bone formation). Hematoxylin and eosin staining was performed for group (A) transglutaminase-crosslinked gelatin gel (Tg-Gel), (B) Tg-Gel + 200 ng BMP-2 and (C) Tg-Gel + 500 ng BMP-2 (magnification: 20×). Bone formation and tissue reorganization in the boxed areas of (A–C) are shown with higher magnification in (D–F), respectively.